Mon. Not. R. Astron. Soc. **000**, 1–7 (1999) Printed 10 January 2000 (MN LaTeX style file v1.4)

Hydrogen recombination lines from the Gum nebula

Beate Woermann[1,2]*, Michael J. Gaylard[2] and Robina Otrupcek[3]
[1] *Department of Physics & Electronics, Rhodes University, Grahamstown 6140, South Africa*
[2] *Hartebeesthoek Radio Astronomy Observatory, PO Box 443, Krugersdorp 1740, South Africa*
[3] *Australia Telescope National Facility, PO Box 76, Epping, NSW 2121, Australia*

Accepted 1999 . Received 1999 ; in original form 1999

ABSTRACT

Hydrogen recombination lines in the H156α and H139α transitions have been detected at four widely separated positions in the Gum nebula. This confirms that the radio continuum emission seen in parts of the nebula is predominantly Brehmsstrahlung rather than synchrotron emission.

The derived electron temperatures and emission measures are in the range 4200 to 8500 K and 220 to 470 pc cm^{-6} respectively. This is consistent with the presence of a low density, photoionised plasma. The line width observed at the position away from the edge of the nebula is significantly larger than those near the edge of the nebula. Together with the negative line velocity observed at this position, this suggests there is systematic expansion of the near side of the nebula.

Key words: ISM: individual: Gum nebula – ISM: HII regions – ISM: supernova remnants

1 INTRODUCTION

The Gum nebula is a large, diffuse emission region centred on G258−2, with a radius of 18° (Gum 1952, 1955, 1956; Chanot & Sivan 1983). The nebula evidently originated as a single old supernova remnant (Reynolds 1976b; Duncan et al. 1996) or as a supershell resulting from multiple supernovae (McCray 1988; Reynoso & Dubner 1997). The presence of a thermal component would then be unexpected.

Duncan et al. (1996) showed that the continuum radio emission of the nebula near the galactic plane has a polarized component at positions lacking in Hα emission, suggesting that there is a mixture of nonthermal and thermal radiation. The detection of hydrogen recombination lines from the nebula at radio frequencies would confirm the presence of the suggested thermal radio emission.

In addition, observations, particularly of optical emission and absorption lines, indicate that a wide range of temperatures is apparently present in the ionised gas of the nebula, and there is conflicting evidence regarding the expansion of the nebula. Physical parameters of photoionised regions, such as the electron temperature, emission measure, radial velocity and turbulence, can easily be determined if hydrogen recombination lines can be detected at radio frequencies. The detection of these lines has not previously been reported owing to the observational problem of the very low surface brightness of the nebula. The primary aim of this work therefore was to attempt to detect such recombination lines.

In section 2 we discuss the choice of regions to observe and the observations made with the Mopra antenna of the ATNF. Section 3 covers the results of H156α and H139α recombination line observations at six positions. The derivation of physical parameters from the detected lines and their significance is covered in section 4.

2 OBSERVATIONS

Even the brightest regions of the Gum nebula produce very weak radio emission. Peak continuum antenna temperatures, T_{AC}, of ∼200 mK are found from the Rhodes University/HartRAO 2326 MHz Southern Sky Survey, which has a resolution of 0.33° (Jonas, Baart & Nicolson 1998) (see Fig. 1). For such an antenna temperature the radiometer sensitivity equation implies that 40 hours of integration would be required for the detection of a hydrogen recombination line, assuming a line width, Δv, of 30 km s^{-1} and an electron temperature, T_e, of 10 000 K.

An initial observation attempt in the H142α transition with the HartRAO telescope at 2272.661 MHz (Woermann 1988) using frequency switching failed to produce an unambiguous result. A second attempt was then made using the Mopra telescope, where dual polarization provided improved sensitivity. Frequency switching was also used for the observations at Mopra, where two observing runs were made.

* E-mail: beate@bootes.hartrao.ac.za

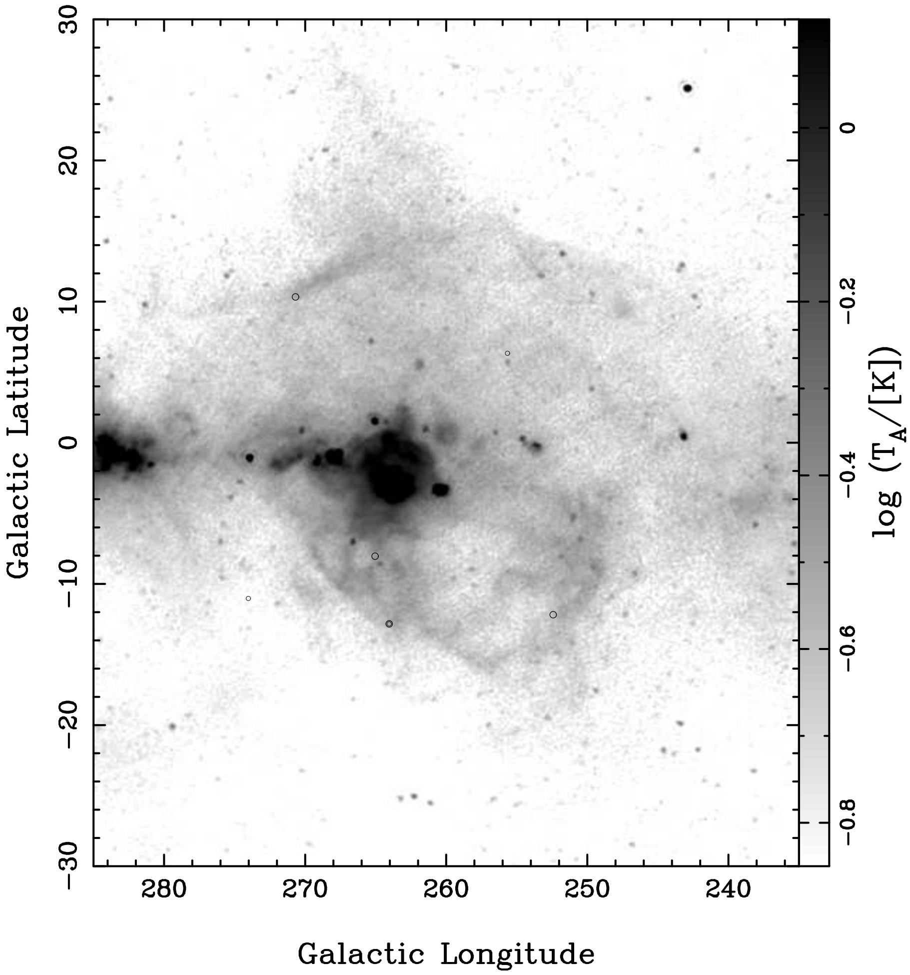

Figure 1. The observed H recombination line positions are shown as circles on the Rhodes University/HartRAO 2.3 GHz map (Jonas, Baart & Nicolson 1998) of the Gum Nebula. The larger circles represents the halfpower beamwidth of the Mopra antenna at 18cm. The smaller circles represent that at 13cm.

The first observing run at Mopra was carried out in April 1994. The H156α transition at 1715.67 MHz was used as this part of the L band then showed the lowest man-made interference levels. The 20 cm receiver system provided simultaneous left- and right-hand circular polarizations. The average zenith system temperature was 34 K at 1665 MHz for both polarizations. The point source sensitivity was 12.7 Jy K^{-1}, as measured on Virgo A (A. Tzioumis, private communication). At 1665 MHz the halfpower beamwidth of the Mopra antenna is $\sim 33'$.

For this first observing period all observed positions were chosen to have a fairly high continuum antenna temperature at 2.3 GHz. Three of the four positions lie near the edge of the nebula. These sample the material of the nebula at one positive galactic latitude, G270.65+10.4, and at two negative galactic latitudes at both high, G264.0−12.8, and low, G252.36−12.15, longitudes. The fourth position, G265.0−8.0, is away from the edge of the nebula (Fig. 1). The aim was to investigate the line width towards and away from the edges in order to look for evidence of expansion of the nebula.

The observations at G264.0−12.8 and G265.0−8.0 were made at a bandwidth of 8 MHz with 1024 channels per polarization. G252.36−12.15 and G270.65+10.4 were observed with half the resolution in order to reduce the required observation time.

The validity of the detections made in these observations was tested in the second observing run in July 1999. Unfortunately the band around 1715.67 MHz was now so contaminated with interference that another H recombination line had to be used in a cleaner band. The best choice was found to be the H139α line at 2422.463 MHz. As a consistency check on the previous observing run, position G264.0−12.8 was reobserved at this frequency. All spectra in this second observing run were obtained by frequency switching with a bandwidth of 8 MHz and 1024 channels per polarization. The average zenith system temperature was 36 K at 2422 MHz for both polarizations. The point source sensitivity was 16 Jy K^{-1}, as measured on Virgo A. At 2422 MHz the half power beamwidth of the Mopra antenna is $\sim 22'$.

The integration times required for the detection of the

H recombination lines presented here are unusally long. Such long integration times may lead to low intensity instrumental artefacts in the spectra that may be mistaken as a detected line. To test if this is the case, position G274.0−11.0 was observed, which lies just outside the Gum nebula and has a galactic latitude comparable to that of the other observed positions. This position also tests whether such low intensity H recombination lines are ubiquitous in the sky irrespective of the direction pointed at and thus perhaps a local phenomenon not associated with the Gum nebula.

Another position within the Gum nebula, G255.6+6.4, was also observed in this second observing run. At this position Reynolds (1976a) reported a double line in Hα.

3 RESULTS

Recombination lines were detected at all four positions observed in the H156α line during the first observing run (Fig. 2). In the second observing run the H139α line was detected at G264.0−12.8 but not at G274.0−11.0 and G255.6+6.4 (Fig. 3).

The integration times are listed in Table 1. The velocity ranges of the spectra from the first and second observing run were approximately -120 km s^{-1} to $+120$ km s^{-1} and -90 km s^{-1} to $+90$ km s^{-1} respectively for fitting polynomials to remove baseline curvature. The orders of polynomials fitted to the baselines, excluding the sections where the lines were visible, are listed in Table 1.

The residual noise after baseline subtraction in the spectra is in reasonable agreement with the antenna sensitivity equation for the listed integration times, t, i.e. the noise still decreases as $\sqrt{t}$. As spectra of right-hand-circular and left-hand-circular polarization were observed simultaneously the integration time is double the observation time, except in the case where only the spectrum in one polarization was useable.

Table 1 lists the parameters of detected lines determined from single Gaussian fits to the lines. T_{AL} is the peak line antenna temperature of the fitted Gaussian, V_{lsr} is the velocity with respect to the local standard of rest of the line and Δv is the line full width at half maximum.

4 DISCUSSION

4.1 Validity of the detected lines

Fig. 4 shows the frequency-switched but not yet folded right-hand circular (i), left-hand circular (ii) and combined (iii) polarization spectra obtained at position G264.0−12.8 (a: H156α at 1715.670 MHz and b: H139α at 2422.463 MHz) and G274.0−11.0 (c: H139α at 2422.463 MHz). A linear (i.e. first order) baseline fitted across the velocity range shown was subtracted from the raw spectra.

At position G264.0−12.8 'up' and 'down' lines are seen at both frequencies in the combined as well as individual polarization spectra. Note that even though there is a slight difference in the sensitivity of the two polarizations, the 'up' and 'down' lines are definitely present in both polarizations. Such line pairs are also seen in the other combined polarization H156α spectra that are frequency-switched but not yet folded. An exception is position G252.36−12.15, where only

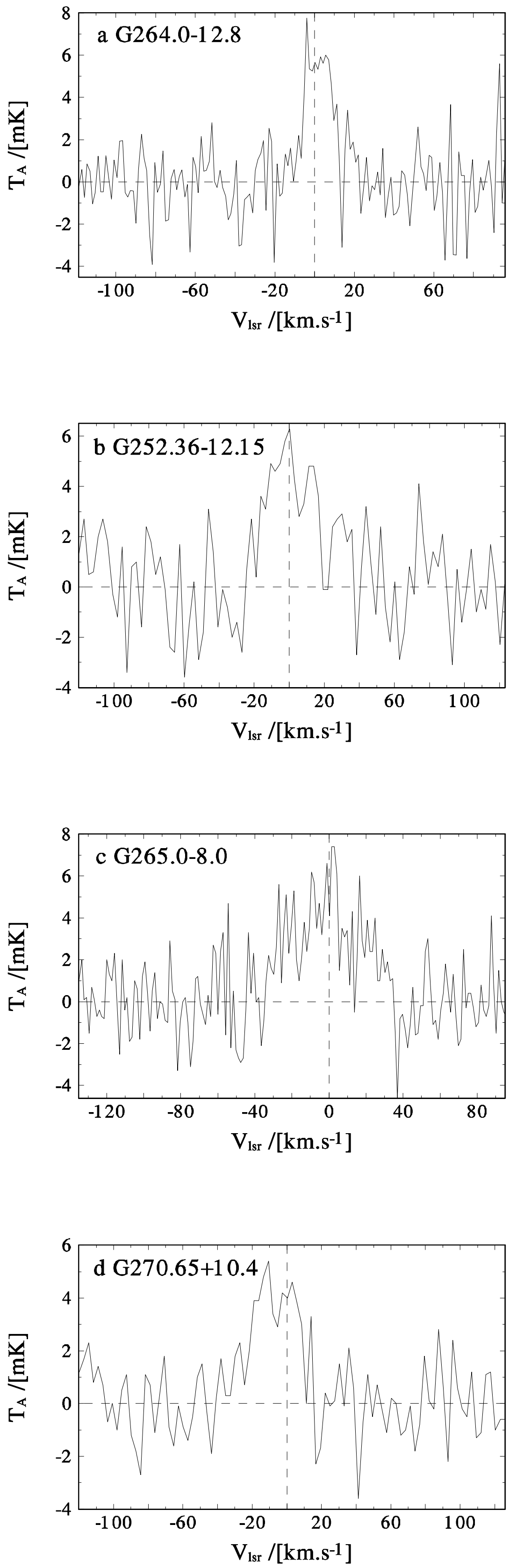

Figure 2. The unsmoothed H156α recombination line spectra obtained at the four positions observed with the Mopra antenna during the first observing run.

Table 1. The positions, integration times, orders of polynomials fitted to the baselines and line parameters of the observed H156α and H139α recombination lines.

Galactic coordinates	freq. MHz	obs. time [hrs]	resoln. [km s^{-1}]	order of polynomial	T_{AL} [mK]	V_{lsr} [km s^{-1}]	Δv [kms^{-1}]	rms noise [mK]	Signal/ noise
G252.36−12.15	1715.670	11.5[a]	3.28	4	5.2 ± 1.1	+0.9 ± 3.5	31.5 ± 8.1	1.8	10.0
G255.60+06.40	2422.463	15	0.97	3	<2.5	-	-	2.1	-
G264.00−12.80	1715.670	22.75	1.64	3	6.4 ± 0.9	+1.9 ± 1.1	16.4 ± 2.9	1.5	14.5
	2422.463	20.7	0.97	2	6.7 ± 1.1	+2.8 ± 1.2	14.6 ± 3.2	2.1	12.2
G265.00−08.00	1715.670	11	1.64	4	4.9 ± 0.6	−2.6 ± 2.5	42.9 ± 5.7	1.7	16.6
G270.65+10.40	1715.670	28	3.28	4	4.7 ± 0.8	−7.8 ± 2.6	30.3 ± 5.7	1.3	11.8
G274.00−11.00	2422.463	26.5	0.97	2	-	-	-	1.7	-

[a] only one polarization as the other one was suffering from instrumental problems.

one polarization showed the 'up' and 'down' lines, due to instrumental problems. The spectra from the problematical polarization were discarded for this position.

As the 'up' and 'down' lines in the spectra on the Gum nebula are separated in velocity by the amount corresponding to the 1 MHz used in the frequency switching, we regard the H156α and H139α lines detected at positions on the Gum nebula as real. In contrast, the off-source position G274.0−11.0 clearly shows no 'up' and 'down' lines in any of the three spectra shown in Fig. 4. Thus the low intensity recombination lines detected at four positions on the Gum nebula originate within the nebula and are not a local ubiquitous or intrumental phenomenon.

The agreement between the H156α and H139α line parameters observed at G264.0−12.8 is good, given the uncertainties in these parameters. This also demonstrates that the apparent lines are extremely unlikely to be due to interference, which would not replicate identically at two quite different frequencies.

The non-detection of a line at G255.6+6.4 could be due to the relatively short observing time of 15 hrs combined with the rather low continuum antenna temperature at this position (see Table 2). By contrast, the line at position G264.0−12.8 was already clearly visible after 15 hrs observation time. An alternative explanation for this non-detection is that the radio continuum emission at G255.6+6.4 is not primarily due to brehmsstrahlung, but rather to synchrotron radiation. This is consistent with the discovery of Duncan et al. (1996) that there is a mixture of nonthermal and thermal radiation in the Gum nebula. The double Hα line detected at this position by Reynolds (1976a) thus originates in hot gas now cooling and recombining, rather than in photoionised gas. This supports the model of Reynolds (1976b) in which the neutral shell around an old supernova remnant is partially ionised by OB stars in the interior. In such a scenario the optical Hα line emission may originate in either the hot SNR gas now cooled to a level where sufficient Hα occurs, or from the photoionised gas of the neutral outer shell.

4.2 Determination of the continuum antenna temperatures

The detection of the hydrogen recombination lines at Mopra meant that continuum antenna temperatures, T_{AC}, at the source positions, obtained with the same system at the same frequency, were required to calculate the electron temperatures. As the newly commissioned Mopra antenna was running on a trial basis at the time of our first observations, the necessary software for such measurements was not yet available. Thus continuum antenna temperatures for the H156α lines were estimated using the 2326 MHz Rhodes University/HartRAO (Jonas et al. 1998) continuum map of the region, convolved to 0.5° resolution. The continuum antenna temperatures for the H139α line were estimated from the same survey at its original resolution of 20′. The antenna temperatures at the line frequency were scaled from the 2326 MHz values by assuming a spectral index of 2.1. The higher efficiency of the Mopra antenna was assumed to compensate for its smaller collecting area compared to the HartRAO antenna. The estimated continuum antenna temperatures are listed in Table 2. The continuum temperatures thus determined may overestimate the thermal component, as Duncan et al. (1996) showed that the radiation of the Gum nebula near the plane is a combination of thermal and nonthermal emission, a scenario that is likely to extend to regions further from the plane.

4.3 Electron Temperatures

The electron temperatures, T_e, were determined from

$$T_e = \left(6350\ \nu_{GHz}^{1.1}\ T_{AC}\ /\ (T_{AL}\ \Delta v)\right)^{0.87}\ \ \mathrm{K} \qquad (1)$$

where ν_{GHz} is the line frequency in GHz (Brown, Lockmann & Knapp 1978). For the five observed positions this gives the values listed in Table 2.

At G264.0−12.8 the electron temperatures calculated from the two different H recombination lines agree fairly well. However this electron temperature is ∼3000 K higher than the average of ∼5000 K obtained at the other positions. This difference is discussed in section 4.4.

How do these values compare to previous measurements? The electron temperatures derived from the spectra are in the accepted range for thermal radio emission from low density HII regions in the solar neighbourhood (Gaylard 1984; Gaylard & Kemball 1984).

Several values of T_e for the nebula have been obtained from low frequency radio continuum data. From the absorption of background radiation by the Gum nebula, using an emission measure $\leq$ 300 pc cm^{-6}, T_e was found to be 8500 $^{+4500}_{-3500}$ K (Beuermann 1973). Other radio absorption calculations, based on overestimated emission measures ($\geq$

Table 2. Parameters derived from the H156α and H139α recombination lines.

Galactic coordinates	freq. [MHz]	T_{AC} [mK]	T_e [K]	$< v_t >$ [km s^{-1}]	EM [pc cm^{-6}]
G252.36$-$12.15	1715.670	210 $\pm$ 40	4200 $\pm$ 1400	20.8 $\pm$ 6.7	220 $\pm$ 60
G255.60+06.40	2422.463	60 $\pm$ 30	>3900[a]	-	>130
G264.00$-$12.80	1715.670	300 $\pm$ 70	8500 $\pm$ 2400	undefined	400 $\pm$ 120
	2422.463	175 $\pm$ 35	7800 $\pm$ 2300	undefined	470 $\pm$ 130
G265.00$-$08.00	1715.670	380 $\pm$ 80	5700 $\pm$ 1400	29.2 $\pm$ 4.6	440 $\pm$ 110
G270.65+10.40	1715.670	265 $\pm$ 60	5800 $\pm$ 1700	18.8 $\pm$ 5.1	310 $\pm$ 90

[a] assuming a line width of 30km s^{-1}.

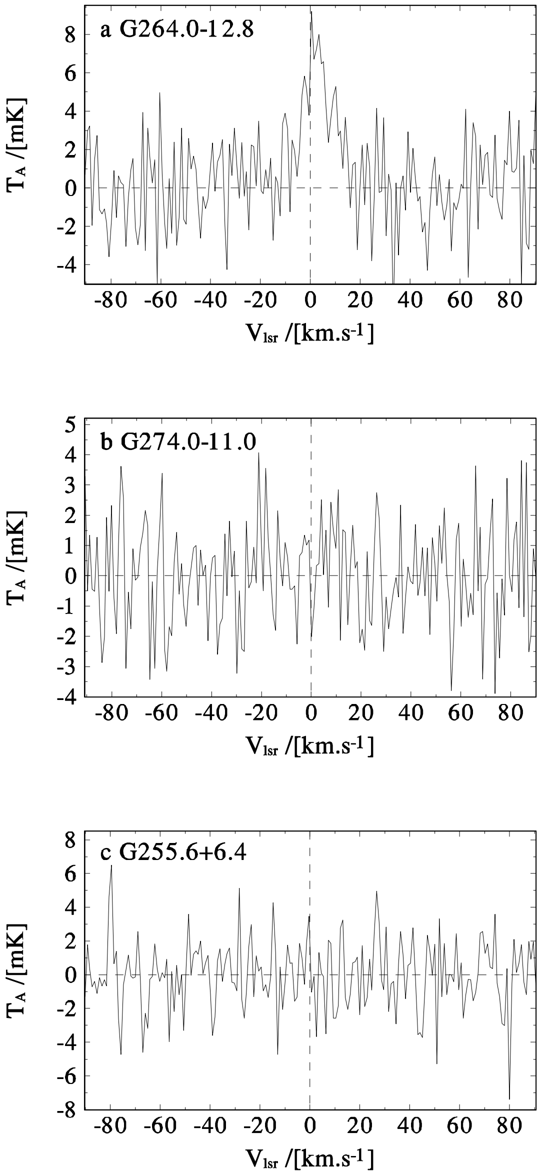

Figure 3. The unsmoothed H139α recombination line spectra obtained at the three positions observed with the Mopra antenna during the second observing run.

600 pc cm^{-6}), gave $T_e > 10^4$ K (Alexander et al. 1971; Ellis 1972; Cane 1973).

Optically derived temperatures are usually higher than those found from the radio recombination lines, as optical emission lines are strongest from the hottest parts of an HII region, whereas radio Hnα lines preferentially sample the cooler parts, and this is evidently the case here as well. For example, Reynolds (1976a) found temperatures ranging from 3 000 to 17 000 K, with an average of 11 300 K, while Chanot & Sivan (1983) obtained an average value of 8 000 K and Srinivasan Sahu & Sahu (1993) found a range from 5 000 to 12 000 K.

Far higher values of T_e come from the highly ionised atoms identified in UV absorption spectra towards the stars thought to ionise the gas, with $T_e > 10^5$ K towards γ^2 Velorum and ζ Puppis (Morton 1978; Bruhweiler, Kondo & McCluskey 1979; Morton & Bhavsar 1979). Bruhweiler et al. (1979) also presented evidence for intermediate temperatures (35 000 K $< T_e <$ 63 000 K).

The large range of temperatures is in keeping with the model of the Gum nebula as a complex object combining HII region and SNR properties (Reynolds 1976b; Burton, Evans & Griffin 1974; Srinivasan Sahu & Sahu 1993; Duncan et al. 1996; Reynoso & Dubner 1997; Woermann, 1997).

4.4 Turbulence and systematic motions

The observed line width is the product of the instrumental resolution, the thermal width of the line, pressure broadening, turbulence and systematic motions. The instrumental broadening is accounted for during data reduction. In this extended, low density nebula, pressure broadening should be negligible at this frequency, so the line will have a Gaussian profile. Hence, for a hydrogen recombination line the thermal and turbulent contributions to the full width at half maximum of the line are given by

$$\Delta v = \sqrt{1.85 < v_t >^2 + 0.0457\ T_e} \qquad \mathrm{km\ s^{-1}} \qquad (2)$$

where $< v_t >$ is the rms turbulent velocity, which encompasses both turbulence and systematic motions (Kardashev 1959; Reifenstein et al. 1970).

The turbulent velocities derived from equation (2) above are listed in Table 2. At G264.0$-$12.8 the derived electron temperature combined with the measured line width in equation 2 implies that the derived electron temperature is invalid as the thermal width at $\sim$8000 K exceeds that given by the measured line width. The thermal line width, given

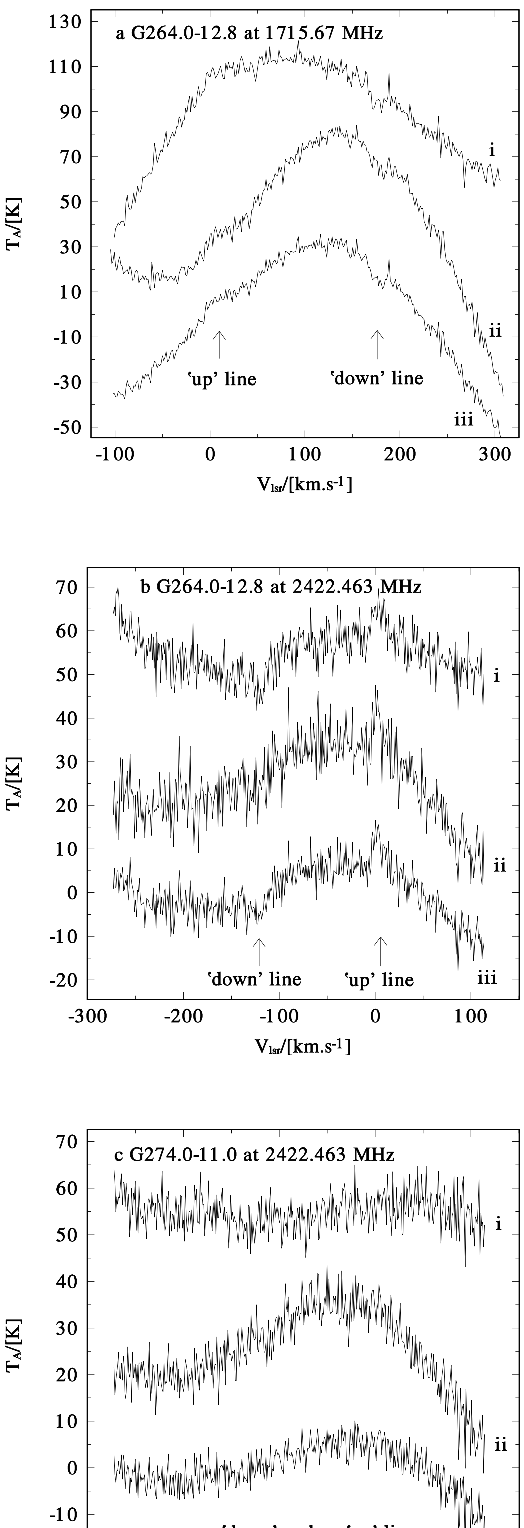

Figure 4. The frequency-switched but not yet folded right-hand circular (i) left-hand circular (ii), and combined (ii) polarization spectra obtained at position G264.0−12.8 in the a H156α line at 1715.67 MHz and b H139α line at 2422.463 MHz and at position G274.0−11.0 in the c H139α line at 2422.463 MHz .

an electron temperature of 5000 K as derived at the other positions, is $\sim$15 km s^{-1}, i.e. equal to the measured line width at G264.0−12.8, given the uncertainties. As it is unlikely that there is no turbulence present at G264.04−12.8, we derived the expected electron temperature assuming a conservative value of 10 km s^{-1} for the tubulent velocity and using the measured line width. This implies an electron temperature of $\sim$900 K, significantly lower than that obtained at the other positions.

The contradiction in electron temperature implied by the measured line parameters at G264.0−12.8 can be explained if the continuum antenna temperature at this position is only partly due to brehmsstrahlung. An electron temperature of $\sim$3000 K and a turbulent velocity of 10 km s^{-1} imply a line width of $\sim$17 km s^{-1}. This is within the error on the measured line width at this position.

The figures at the other positions are typical for HII regions. From optical line data Srinivasan Sahu & Sahu (1993) derived values of 14 to 17 km s^{-1} for $< v_t >$ at eight positions within the nebula. These are consistent with three of the four values found here. A significantly broader line was observed at G265.0−8.0, away from the edge of the nebula. If physical conditions are similar at all four positions, this excess line broadening could be explained as due to systematic expansion of the nebula.

Some investigators have reported no evidence for expansion of the nebula (Hippelein & Weinberger 1975; Wallerstein, Silk & Jenkins 1980; Zealey et al. 1983). Srinivasan Sahu & Sahu (1993) found that only part of the nebula is expanding, at 10 ± 2 km s^{-1}, and identified this as a separate structure, the IRAS Vela Shell. The centre of this proposed structure is at G263−7, very close to the position at which the broadest recombination line was observed. However, Reynolds (1976a) reported that five of seven positions within the nebula, including some outside this structure, show two peaks in the Hα line separated by 20 to 45 km s^{-1}, indicating an expansion of $\sim$20 km s^{-1}. Sridharan (1992) showed that CO line velocities of cometary globules embedded in the nebula imply an expansion velocity of 12 km s^{-1}. The latter sets a lower limit to the expansion velocity of the ionised gas. The data presented here are suggestive of expansion of the nebula, but do not cover sufficient directions to distinguish between general expansion and that of a substructure such as the IRAS Vela Shell.

4.5 Line velocities and the kinematic distance

The H156α and H139α line velocities at G252.36−12.15, G264.0−12.80 and G270.65+10.40 listed in Table 1 agree with nearby Hα and NII measurements (Hippelein & Weinberger 1975; Srinivasan Sahu & Sahu 1993), within the errors. However, the close proximity of the Gum nebula to us means that kinematic distances are poorly constrained and peculiar motions may dominate the observed line velocity. At best, the observed line velocities place the kinematic distance to the emission regions as within 1 kpc.

Reynoso & Dubner (1997) identified a 34°-diameter HI disk lying in the direction of the Gum nebula. This neutral gas has a velocity range of 0 to +10 km s^{-1}, and so must lie behind the Gum nebula. It probably encloses the far side of the nebula and constrains its expansion.

The near side of the nebula is very close to us. From stellar reddening data, Franco (1990) obtained a distance of 200 ± 20 pc for the near edge of the nebula in the vicinity of G258.4−11.1 and G271.3+5.3. Hipparcos parallax measurements yield a distance of 258^{+41}_{-31} pc to γ^2 Velorum and 429^{+120}_{-77} pc to ζ Puppis (Schaerer, Schmutz & Grenon 1997, van der Hucht et al. 1997). These stars are considered to be within the nebula. Excluding systematic motions, gas on the near side of the nebula should have lsr velocities close to zero. The negative velocity recorded at G265.00−8.00 suggests that this gas lies on the near side of the nebula and that the near side is expanding towards us.

4.6 Emission measures

The emission measure (EM) at frequency ν may be derived from the electron and brightness temperatures, T_b, at the observed hydrogen recombination line positions using the relation (Mezger & Henderson, 1967):

$$EM = 12.14\ T_e^{0.35}\ \nu_{GHz}^{2.1}\ T_b \tag{3}$$

In calculating the emission measures listed in Table 2, we assume that the conversion factors from T_A to T_b for the Mopra and HartRAO antennas are the same, namely 1.5.

Reynolds (1976a) published Hα-derived emission measures for the Gum nebula. After revision of the calibration (Reynolds, private communication), these range from 8 to 320 pc cm^{-6}. A similar range was reported by Chanot & Sivan (1983), with an average of about 100 pc cm^{-6}. The highest optically derived emission measures agree with those derived from the radio line and continuum data, as expected, given that most of the radio observations were made at positions chosen for their high radio brightness temperatures.

5 CONCLUSIONS

This first detection of hydrogen recombination lines at four positions in the Gum nebula shows that the radio emission at these positions is primarily due to thermal rather than synchrotron emission. The non-detection of a line at one other position may be an indication that synchrotron emission dominates at that position. This is in agreement with the results of Duncan et al. (1996) that the Gum nebula is a mixture of thermal and nonthermal emission.

The presence of thermal emission consistent with photoionization points to the mixed origins of the Gum nebula. It supports models in which an old SNR or superbubble is surrounded by an HII shell, as first proposed by Reynolds (1976b).

Reynoso & Dubner (1997) showed that the back face of the Gum nebula is surrounded by a neutral hydrogen shell. The thermal component could then be explained as either:

- Regions of gas heated in the shock front but now cooled sufficiently to emit thermal rather than nonthermal radiation. Such cooled regions could now be maintained as HII regions by the Lyman continuum flux from the stars ζ Puppis and γ^2 Velorum that appear to be located within the nebula, as suggested by Reynolds (1976b);
- Neutral material outside the supershell that has been ionised by the Lyman continuum flux from the same stars and other OB stars within the neutral shell (McCray 1988; Reynoso & Dubner 1997).

It has not been possible to distinguish between these scenarios for the creation of the thermal emission regions on the basis of current evidence.

The line velocities are consistent with previous estimates of the distances to the near and far sides of the nebula, and suggest that expansion of the nebula is constrained on the far side but is occuring relatively freely on the near side. The large line width and negative velocity observed at G265.0−8.0, away from the edge of the nebula, supports this interpretation.

The derived electron temperatures of 4200 to 8500 K and emission measures of 220 to 470 pc cm^{-6} agree with values determined from low frequency radio absorption and from optical emission lines.

ACKNOWLEDGMENTS

We thank the referee for helpful comments.

REFERENCES

Alexander J.K., Brandt J.C., Maran S.P., Stecher T.P., 1971, ApJ, 167, 487
Beuermann K.P., 1973, Ap&SS, 20, 27
Brown R.L., Lockman F.J., Knapp G.R., 1978, ARA&A, 16, 445
Bruhweiler F.C., Kondo Y., McCluskey G.E., 1979, ApJ, 229, L39
Burton W.M., Evans R.G., Griffin W.G., 1974, MNRAS, 169, 307
Cane H.V., 1973, Proc. ASA 2 (4), 197
Chanot A., Sivan J.P., 1983, A&A, 121, 19
Duncan A.R., Stewart R.T., Haynes R.F., Jones K.L., 1996, MNRAS, 280, 252
Ellis G.R.A., 1972, Proc. ASA 2 (3), 158
Franco G.A.P., 1990, A&A, 227, 499
Gaylard M.J., 1984, MNRAS, 211, 149
Gaylard M.J., Kemball A.J., 1984, MNRAS, 211, 155
Gum C.S., 1952, Observatory, 72, 151
Gum C.S., 1955, Mem. RAS, 67, 155
Gum C.S., 1956, Observatory, 76, 150
Hippelein H.H., Weinberger R., 1975, A&A, 43, 405
Jonas J.L., Baart E.E., Nicolson G.D., 1998, MNRAS, 297, 977
Kardashev N.S., 1959, Soviet Astron.-AJ, 3, 813
McCray R., 1988, in Roger R.S., Landecker T.L., eds, IAU Coll. 101, Supernova Remnants and the Interstellar Medium. Cambridge University Press, Cambridge, p. 447
Mezger P.G., Henderson A.P., 1967, ApJ, 147, 471
Morton D.C., 1978, ApJ, 222, 863
Morton D.C., Bhavsar S.P., 1979, ApJ, 228, 147
Reifenstein III E.C., Wilson T.L., Burke B.F., Mezger P.G. & Altenhoff W.J., 1970, A&A, 4, 357
Reynolds R.J., 1976a, ApJ, 203, 151
Reynolds R.J., 1976b, ApJ, 206, 679
Reynoso E.M. & Dubner G.M., 1997, A&AS, 123, 31
Schaerer D., Schmutz W., Grenon M., 1997, ApJ, 484, L153
Sridharan T.K., 1992, JA&A, 13, 217
Srinivasan Sahu M., Sahu K.C., 1993, A&A, 280, 231
van der Hucht et al., 1997, New Astronomy, 2, 245
Wallerstein G., Silk J., Jenkins E.B., 1980, ApJ, 240, 834
Woermann B., 1988, MNASSA, 47, 28
Woermann B., 1997, Ph.D. thesis,'Radio Observations of the Gum Nebula Region', Rhodes University, Grahamstown, South Africa
Zealey W.J., Ninkov Z., Rice E., Hartley M., Tritton S.B., 1983, Ap. Let., 23, 119